Free Radical Biology and Medicine XX

Contents lists available at ScienceDirect

Free Radical Biology and Medicine

journal homepage: www.elsevier.com/locate/freeradbiomed

Original Contributions

Ferritin heavy chain as main mediator of preventive effect of metformin against mitochondrial damage induced by doxorubicin in cardiomyocytes

Mari C. Asensio-Lopez [a,b,1], Jesus Sanchez-Mas [a,b,1], Domingo A. Pascual-Figal [a,b], Carlos de Torre [c], Mariano Valdes [a,b], Antonio Lax [a,b,*]

[a] Cardiology Department, University Hospital Virgen de la Arrixaca, 30120 Murcia, Spain
[b] Department of Medicine, School of Medicine, University of Murcia, 30120 Murcia, Spain
[c] Research Unit, University Hospital Virgen de la Arrixaca, 30120 Murcia, Spain

ARTICLE INFO

Article history:
Received 18 April 2013
Received in revised form
21 October 2013
Accepted 5 November 2013
Available online XX

Keywords:
Cardiotoxicity
Doxorubicin
Metformin
Ferritin
Iron homeostasis
Mitochondrial function
Free radicals

ABSTRACT

The efficacy of doxorubicin (DOX) as an antitumor agent is greatly limited by the induction of cardiomyopathy, which results from mitochondrial dysfunction and iron-catalyzed oxidative stress in the cardiomyocyte. Metformin (MET) has been seen to have a protective effect against the oxidative stress induced by DOX in cardiomyocytes through its modulation of ferritin heavy chain (FHC), the main iron-storage protein. This study aimed to assess the involvement of FHC as a pivotal molecule in the mitochondrial protection offered by MET against DOX cardiotoxicity. The addition of DOX to adult mouse cardiomyocytes (HL-1 cell line) increased the cytosolic and mitochondrial free iron pools in a time-dependent manner. Simultaneously, DOX inhibited complex I activity and ATP generation and induced the loss of mitochondrial membrane potential. The mitochondrial dysfunction induced by DOX was associated with the release of cytochrome *c* to the cytosol, the activation of caspase 3, and DNA fragmentation. The loss of iron homeostasis, mitochondrial dysfunction, and apoptosis induced by DOX were prevented by treatment with MET 24 h before the addition of DOX. The involvement of FHC and NF-κB was determined through siRNA-mediated knockdown. Interestingly, the presilencing of FHC or NF-κB with specific siRNAs blocked the protective effect induced by MET against DOX cardiotoxicity. These findings were confirmed in isolated primary neonatal rat cardiomyocytes. In conclusion, these results deepen our knowledge of the protective action of MET against DOX-induced cardiotoxicity and suggest that therapeutic strategies based on FHC modulation could protect cardiomyocytes from the mitochondrial damage induced by DOX by restoring iron homeostasis.

© 2013 Elsevier Inc. All rights reserved.

Anthracyclines such as doxorubicin (DOX) are widely used as antitumor drugs. However, a major limitation to their use is the development of cardiomyopathy at high cumulative doses, which finally leads to congestive heart failure [32,35]. DOX cardiotoxicity typically occurs at an average total dose of 500 mg/m^2, although recent studies have shown that such cardiotoxicity may appear at doses as low as 300 mg/m^2 [40,46]. In addition, chemotherapy-induced cardiomyopathy is becoming more prevalent because heart failure in DOX-treated patients can go undetected for between 4 and 20 years after the cessation of treatment and long-term cancer survivors are increasing in numbers [43]. Because dose-limitation strategies have failed to eliminate the risk of DOX cardiotoxicity, considerable research has focused on the search for new drugs able to prevent the cardiotoxic effects of DOX without interfering with its ability to kill cancerous cells [19,26,53]. Nevertheless, to date, only the iron chelator dexrazoxane has been approved as a preventive strategy for DOX cardiotoxicity [19].

Mitochondria are believed to be the main target of the cardiotoxicity induced by DOX, which causes morphological and

Abbreviations: ΔΨm, mitochondrial membrane potential; CCCP, carbonyl cyanide *m*-chlorophenylhydrazone; DOX, doxorubicin; EDTA, ethylenediaminetetraacetic acid; FHC, ferritin heavy chain; HBSS, Hanks' balanced salt solution; MET, metformin; MPTP, mitochondrial permeability transition pore; NF-κB, nuclear factor κB; PBS, phosphate-buffered saline; PMSF, phenylmethylsulfonyl fluoride; ROS, reactive oxygen species; RPA, rhodamine B–[(1,10-phenanthrolin-5-yl)aminocarbonyl]benzyl ester; RPAC, rhodamine B–4-[(phenanthren-9-yl)aminocarbonyl]benzyl ester; TNFα, tumor necrosis factor-α; TUNEL, terminal deoxynucleotidyl transferase dUTP nick-end labeling

* Corresponding author at: University Hospital Virgen de la Arrixaca, Cardiology Department, Ctra. Madrid-Cartagena s/n, 30120 Murcia, Spain.
Fax: +34 868 888115.
E-mail address: alax@um.es (A. Lax).

[1] These authors contributed equally to this work.

0891-5849/$ - see front matter © 2013 Elsevier Inc. All rights reserved.
http://XX

functional alterations in the mitochondrial structure of the heart [38,50]. The primary effect of DOX on mitochondrial performance is its interference with the respiratory chain and oxidative phosphorylation, leading to increased oxidative stress, the depletion of cellular reducing equivalents, and the inhibition of ATP synthesis [16,47]. The altered redox status is believed to cause the induction of the mitochondrial permeability transition pore and the complete loss of mitochondrial integrity and function [30]. If taken to an extreme, this loss of mitochondrial plasticity may lead to the release of signals that mediate cardiomyocyte apoptosis, leading to progressive cardiomyocyte death and the development of congestive heart failure. Although the precise mechanisms involved in DOX-induced mitochondrial dysfunction are not completely understood, iron-mediated free radicals are thought to be primarily responsible [32,42]. The redox state of iron can be converted between the iron(II) and the iron(III) states by interaction with DOX, generating toxic reactive oxygen species (ROS). Iron is an essential trace element for proper cell functioning, but an excess generates oxidative stress and profound cellular toxicity [42,51]. To avoid this toxic effect, any excess of intracellular iron is sequestered by the ferritin heavy chain (FHC), the subunit of ferritin responsible for intracellular iron storage [48]. In cardiomyocytes, the DOX-induced increase in ROS has been associated with FHC upregulation, which seems to be a physiological defensive response to compete with the binding of DOX with iron and so reduce its cardiotoxicity [9]. In this sense, FHC-knockout mice are more susceptible to damage induced by DOX and have increased mortality after chronic DOX treatment compared with wild-type mice [34]. Therefore, iron homeostasis and the modulation of FHC seem to play a key role in DOX-induced mitochondrial dysfunction in the cardiomyocyte.

Metformin (MET) is an oral antihyperglycemic biguanide, widely used for the management of type 2 diabetes, which has also been seen to reduce the risk of all-cause mortality and myocardial infarction in patients with type 2 diabetes [1,2]. It has also been seen to reduce mortality in diabetic patients with heart failure [13,41]. MET has an important antioxidant activity in cardiomyocytes, reducing the generation of ROS in animal models of heart failure [18,39] and protecting cardiomyocytes from the oxidative stress induced by H_2O_2 or TNFα [27,39]. Our group has recently reported the ability of MET to prevent oxidative stress and cell death induced by DOX in cardiomyocytes [4]. In addition, we identified NF-κB-mediated FHC upregulation as the main mechanism responsible for the protective effect of MET against DOX-induced cardiotoxicity [5]. The modulation of FHC induced by MET suggests a role for the biguanide in preserving cardiac iron homeostasis and therefore in preserving mitochondrial function. A recent study in a rat model of DOX-induced cardiotoxicity suggested that the protective role of MET involves reversing the ultrastructural deterioration of mitochondria induced by the anthracycline and restoring DOX-induced energy starvation [6]. However, the mechanisms involved in this protective role of MET remain unclear. In light of all the above, this study aimed to assess the protective role of MET against the DOX-induced loss of iron homeostasis and mitochondrial dysfunction in cardiomyocytes and the involvement of NF-κB and FHC in this effect.

Materials and methods

Reagents

DOX, MET, Claycomb medium, fetal bovine serum, protease inhibitor cocktail, L-glutamine and penicillin–streptomycin mixture, (±)-norepinephrine (+)-bitartrate salt, phenylmethylsulfonyl fluoride (PMSF), and other biochemicals were obtained from Sigma–Aldrich Corp. (St. Louis, MO, USA). The ECL immunoblot detection reagents and prestained molecular weight markers were from Amersham Pharmacia Biotech (Piscataway, NJ, USA).

Cell culture, treatments, and preparation of cell extracts

HL-1 cells are a cardiac muscle cell line derived from the AT-1 mouse atrial cardiomyocyte tumor lineage, which contracts and retains phenotypic characteristics of the adult cardiomyocyte. HL-1 cells were a kind gift from Dr. W.C. Claycomb (Louisiana State University Medical Center, New Orleans, LA, USA). Cells were maintained in exponential growth phase as previously described [5]. All the experiments were conducted in the absence of fetal bovine serum and antibiotics. For the induction of cardiotoxicity, plated cells were exposed to 5 μM DOX for the indicated treatment times. The dosage of DOX was selected according to previous assays [4,5] and reproduces the plasma peak concentration reached by standard infusions in patients [15]. The MET concentration selected was 4 mM, which represents the physiological dose [36]. For cell extracts, cells were harvested with trypsin/EDTA, washed with phosphate-buffered saline (PBS), and solubilized in 10 mM Tris–HCl, pH 7.4, 1% Triton X-100 (v/v) and 0.1 mM PMSF. Samples were centrifuged at 10,000 *g* for 20 min at 4 °C. The supernatant was aliquotted and stored at −80 °C for further study. The isolation of cytosolic and mitochondrial samples was based on a previously described method for selective permeabilization of the plasma membrane [44]. Briefly, cells were collected by centrifugation, washed twice in ice-cold PBS, and resuspended at $\sim 4 \times 10^4$ cells/μl in ice-cold medium for permeabilization: 75 mM KCl, 1 mM NaH_2PO_4, 8 mM Na_2HPO_4, and 250 mM sucrose, pH 7.4. The protease inhibitor cocktail at 4 μl/1 $\times 10^6$ cells and an amount of digitonin to give 600 μg/ml were added. The incubation was maintained for 5 min in an ice bath. Cells were centrifuged at 10,000 *g* for 10 min and at 4 °C and the supernatant was stored at −80 °C in the bank of samples. The pellet was resuspended in a volume of solubilization buffer equal to the volume of medium previously used for permeabilization. The addition of protease inhibitor cocktail at 4 μl/1 $\times 10^6$ cells and a brief sonication (4–5 s with 30-s intervals) at ice-water temperature were followed by a new centrifugation step at 10,000 *g*. The resulting supernatant was aliquotted and frozen at −80 °C. The protein content of the supernatants was determined by the bicinchoninic acid method.

Primary neonatal rat cardiomyocyte isolation

A primary culture of neonatal rat cardiomyocytes was isolated using the neonatal cardiomyocyte isolation system (NCIS) purchased from Worthington Biochemical Corp. (Lakewood, NJ, USA). Briefly, primary cardiomyocyte cultures were prepared from ventricles of 3-day-old Wistar rats. The hearts from 6 to 10 rats were excised, the ventricles pooled, and the ventricular cells isolated according to the NCIS protocol. The pups were killed by decapitation with sterile scissors, and their beating hearts were surgically removed and immediately placed in ice-cold Hanks' balanced salt solution (HBSS). Hearts were minced and digested overnight by trypsinization at 4 °C. The following morning, the tissue preparation was digested for 45 min with collagenase, slowly shaking at 3 rpm at 37 °C. Cells were then dispersed by trituration, filtered through a cell strainer, sedimented, and centrifuged at 1000 rpm for 5 min, and the supernatant was removed. Pellets were resuspended in Dulbecco's modified Eagle's medium low-glucose culture medium supplemented with 5% fetal bovine serum, 10% horse serum, 1% L-glutamine, 100 U/ml penicillin, and 100 μg/ml streptomycin. After fibroblast separation, neonatal rat cardiomyocytes were counted, seeded, and subjected to the specific treatment as indicated.

Knockdown with small interfering RNA (siRNA)

To ensure the validity of the data of the knockdown experiments we used a combination of two siRNAs designed against different regions of the same target gene. The siRNAs used to reduce FHC expression were obtained from Ambion (Austin, TX, USA): siRNA FHC-1 (66945, sense, 5′-GGUGAAAUCCAUUAAAGAAtt-3′) and siRNA FHC-2 (158606, sense, 5′-CGUAUUAUCUGAGUGAACAtt-3′). The expression of NF-κB p65 subunit, which is specifically involved in FHC induction [48], was reduced using a combination of two siRNAs from Santa Cruz Biotechnology (Santa Cruz, CA, USA): siRNA NF-κB-1 (sc-44213A, sense, 5′-CCUUUCACGUUCCUAUAGAtt-3′) and siRNA NF-κB-2 (sc-44213B, sense, 5′-CUGUACACCUUGAUCCAAAtt-3′). A negative control siRNA (sense, 5′-AUUUAACUUCUGGUGACGAUACU-3′) synthesized by Bonsai Technologies (Madrid, Spain) was used as control (scramble). SiRNA transfection was performed using Lipofectamine 2000 according to the manufacturer's instructions. Briefly, subconfluent HL-1 cells were plated in six-well plates in complete culture medium. The following day, they were transfected with 50 nM control siRNA or a combination of two siRNAs for each target (50 nM per siRNA) for 8 h followed by recovery in serum-containing medium. Twenty-four hours after siRNA transfection, cultured cells were washed twice with PBS at 37 °C and subjected to the specific treatments as indicated. The effectiveness and specificity of these siRNAs for silencing FHC and NF-κB expression were confirmed in HL-1 cardiomyocytes (supplementary material).

Labile iron pool determination

Cytosolic iron pools were measured as previously described using the iron-sensitive probe calcein-AM [5]. For the measurement of mitochondrial iron pools, HL-1 cells were loaded with 5 μM rhodamine B–[(1,10-phenanthrolin-5-yl)aminocarbonyl]benzyl ester (RPA) for 20 min at 37 °C. Rhodamine B–4-[(phenanthren-9-yl)aminocarbonyl]benzyl ester (RPAC), a fluorescent probe unaffected by iron, was used to normalize mitochondrial rhodamine incorporation [37]. Briefly, HL-1 cells were grown at 37 °C for 4 days in complete culture medium (2×10^6 cells per flask). After the indicated treatment, the cells were washed and loaded with 5 μM RPA or 5 μM RPAC, at 37 °C for 20 min. After two wash cycles with HBSS, cells were maintained in HBSS supplemented with 10 mM glucose. The decrease in fluorescence was used to calculate the increase in the free iron pool. Cell monolayers were harvested by trypsinization (1.5 ml of 0.25% trypsin/EDTA per 10-cm dish) for 3 min at 37 °C. The cells were pelleted by centrifugation and resuspended in Ca^{2+}/Mg^{2+} PBS (0.5 μg/ml each of $CaCl_2$ and $MgCl_2$) at a density of 0.5×10^6 cells/ml. The fluorescence of the cells was monitored with a FLUOstar Omega spectrofluorimeter (λ_{ex} 530 nm; λ_{em} 590 nm). HL-1 cells treated with DOX alone were used to subtract the autofluorescence of DOX (Supplementary Fig. 4). A total of 6×10^5 cells were collected and analyzed. The results are representative of four experiments performed under selected assay conditions. Fluorescence intensity is shown as fold of control (HL-1 cells with RPAC).

Mitochondrial complex I activity assay

Briefly, cells at $\sim 1.5 \times 10^6$ cells/well were seeded in quadruplicate in six-well plates and grown at 37 °C for 2 days in complete culture medium. Subconfluent cultures were subjected to the indicated treatment. Culture medium from treated or untreated cells was aspirated and cells were washed twice with prewarmed PBS. Cells were assayed for complex I activity using the Mitoprofile Complex I Rapid ELISA Kit (MitoSciences, Eugene, OR, USA) according to the manufacturer's instructions. Mitochondrial OXPHOS Complex I was immunocaptured and the activity was determined at 450 nm by following the oxidation of NADH to NAD^+. HL-1 cells treated with DOX alone were used to subtract the intrinsic absorbance value of DOX (Supplementary Fig. 4). Data are depicted as the percentage of activity compared with the control.

Measurement of intracellular adenosine triphosphate levels

Adenosine triphosphate (ATP) was determined using high-performance liquid chromatography (HPLC). HL-1 cells were grown in 75-cm^2 flasks at 37 °C for 2 days in complete culture medium. After the indicated treatment, cells were harvested with trypsin/EDTA and washed with PBS, and 2×10^6 cells were homogenized in 0.2 ml ice-cold 7% perchloric acid for 15 min. Acid-insoluble fractions were removed by centrifugation at 14,000 *g* for 10 min at 4 °C. Supernatant fluid was neutralized with ice-cold 2 M K_2CO_3 and stored at −80 °C until analyzed. The chromatographic separation of ATP was performed using a SUPELCOSIL LC-18-T column (150 mm, 4.6 mm i.d., particle size 3 μm) (Bellefonte, PA, USA). The samples were eluted isocratically for 3.75 min at a flow rate of 1 ml/min with a starting buffer (buffer A) of 100 mM KH_2PO_4 (pH 6.0) that contained 4 mM tetrabutylammonium bisulfate. Then a gradient of buffer A:methanol, 70:30, pH 7.2, was applied for 30 min. The sample injection volume was 0.1 ml and the components were monitored at 254 nm. The ÄKTA Purifier 10 HPLC system (GE Healthcare Life Science, Uppsala, Sweden) was operated at room temperature (23–25 °C). The standard stock solution for calibration curve construction was 10 mM ATP (Sigma) prepared in buffer A. This solution was made fresh before each assay to construct a calibration curve of 0.1, 1, 2.5, and 5 nmol per 0.1 ml injected. Calibration curves were linear over the range assayed. Peaks were identified by comparison with the retention times of standards, as well as by analyses of peak spectra with Unicorn 5.20 software (GE Healthcare Life Science). The ATP concentration (nmol/1×10^6 cells) was determined by measuring the peak area at λ 254 nm and was shown as fold of untreated cells.

Determination of mitochondrial membrane potential ($\Delta\Psi m$)

To examine the change in $\Delta\Psi m$, the JC-1 staining assay was used as previously described [30]. Briefly, treated and untreated cells in Claycomb medium were loaded at 37 °C for 10 min with 5 μg/ml JC-1. After being washed twice with prewarmed PBS, the cells were trypsinized and resuspended at $\sim 3 \times 10^5$ cells/ml in Tyrode's solution at 25 °C. Measurements were immediately made in a FACSort flow cytometer from Becton–Dickinson and samples were excited with the 488-nm line of a krypton/argon laser. JC-1 dye changes its fluorescence emission from red to green when a loss of $\Delta\Psi m$ occurs. The green and red fluorescence of JC-1 was detected through the FL-1 and FL-2 channels, respectively. Proper compensation was established to correct the fluorescence spillover [10]. The cell population under study was previously selected by electronic gating, measuring forward vs side light scatter. A total of 20,000 events were collected for the analysis of each sample. Data acquisition and analysis were performed with the CellQuest software from Becton–Dickinson. Cells with high and low $\Delta\Psi m$ are in regions R1 and R2, respectively. Data are depicted as the percentage of cells in the R1 region compared with untreated cells. The autofluorescence of DOX was subtracted from each measurement (Supplementary Fig. 4). Mitochondrial depolarization was achieved by treating cells with 5 μM CCCP for 30 min at 37 °C and was indicated by a decrease in the red/green fluorescence intensity ratio.

Western blotting

Western blotting was performed as previously described [4]. Briefly, equal amounts of protein were heated to 95 °C, separated by SDS–PAGE on 10% polyacrylamide gels, electrophoretically transferred onto polyvinylidene difluoride membranes (Immobilon-PSQ Membranes; Millipore, Bedford, MA), and blocked in 5% nonfat dry milk in PBS. The primary antibodies used were (reference, dilution factor): anti-cytochrome *c* (556433, 1:500) from BD Pharmingen (San Diego, CA, USA) and anti-caspase 3 (9662, 1:2000) from Cell Signaling (Danvers, MA, USA). Incubation with the primary antibody solution was carried out overnight at 4 °C in a rocker. The binding solution was supplemented with 0.1% Tween 20 (v/v) and 1% nonfat dry milk (p/v). After four washes in washing solution (PBS, 0.1% Tween 20), the membranes were incubated for 60 min at room temperature with the appropriate secondary antibody from Promega (Madison, WI, USA). Immunoreactive bands were detected by ECL using a ChemiDoc XRS+ system with Image Lab software from Bio-Rad Laboratories (Berkeley, CA, USA). A quantitative analysis was performed with Gel-Pro Analyzer 3.1 software (Sigma).

Terminal deoxynucleotidyl transferase dUTP nick-end labeling (TUNEL) assay

Apoptosis is characterized by endonuclease activation leading to DNA fragmentation into segments that can be labeled by immunofluorescent markers. TUNEL assay was carried out using the DeadEnd fluorimetric TUNEL system (Promega) as described in Supplementary Fig. 5. Data are shown as a percentage of TUNEL-positive cells.

Statistical analysis

Experimental data are shown as mean values for at least five independent assays, and standard deviations are indicated by error bars. Differences between groups were tested using Student's *t* test; *p* values of less than 0.05 were regarded as significant. Analyses were carried out using SigmaPlot 11.0 software. Western blots are representative of repeated experiments and were reproduced using the Adobe Photoshop 4.0 software.

Results

MET prevents loss of iron homeostasis induced by DOX

The effects of DOX, MET, and MET + DOX on the cytosolic and mitochondrial free iron pools in cardiomyocytes are shown in Fig. 1. Compared with the control, the treatment of HL-1 cells with DOX diminished the fluorescence intensity in the calcein-AM assays in a time-dependent manner as a result of an increase in the cytosolic free iron pool (Fig. 1A). This decrease in fluorescence intensity was clearly visible after 6 h of exposure to DOX (0.39 ± 0.1-fold of control) and reached the minimum value after 8 h (0.12 ± 0.03). Pretreatment with MET 24 h before the addition of DOX prevented the increase in the cytosolic iron level induced by DOX, whereas MET alone had no effect. Similar behavior was observed in the assays performed to evaluate the effects of DOX, MET, and MET + DOX on the mitochondrial free iron pool (Fig. 1B). Compared with the control, DOX induced a significant decrease in RPA fluorescence as a result of an increase in the mitochondrial free iron pool, which reached a minimum of fluorescence intensity after 6 h of exposure to DOX (0.28 ± 0.1-fold of control). The pretreatment with MET again prevented the increase in mitochondrial free iron induced by DOX, whereas MET alone had no effect. As can be seen from Fig. 1C, FHC and NF-κB are involved in the role played by MET in inhibiting the DOX-induced increase in mitochondrial free iron. Treatment of HL-1 cells with DOX for 6 h significantly decreased the fluorescence intensity as a result of an increase in the mitochondrial free iron pool (0.24 ± 0.08-fold of control, scramble + DOX). As depicted, the increase in mitochondrial iron mediated by DOX was prevented when HL-1 cells were preincubated with MET (0.87 ± 0.1, scramble + MET + DOX). This preventive effect of MET was blocked by the presilencing of FHC expression (0.34 ± 0.03, siRNA FHC + MET + DOX) or NF-κB expression (0.34 ± 0.03, siRNA NF-κB + MET + DOX). The silencing of FHC or NF-κB in the absence of treatment had no effect on the mitochondrial free iron pool compared with the control. FHC or NF-κB silencing combined with DOX did not alter the effect observed with the sole administration of DOX (data not shown). Previous results reported by our group in HL-1 cells showed that MET, through NF-κB-mediated FHC upregulation, is also able to attenuate the increase in the cytosolic free iron pool mediated by DOX [5].

MET prevents mitochondrial dysfunction induced by DOX

To throw light on the role of MET in the mitochondrial dysfunction induced by DOX in cardiomyocytes, the activity of complex I belonging to the mitochondrial electron transport chain was evaluated. Fig. 2A shows the effects of DOX, MET, and MET + DOX on the activity of the complex. As can be seen, the treatment of HL-1 cells with DOX resulted in a time-dependent decrease in complex I activity. The pretreatment with MET prevented DOX-mediated complex I inhibition, whereas MET alone had no effect. Fig. 2B shows how the ability of MET to prevent the inhibition of complex I mediated by DOX (28.3 ± 9.3%, scramble + DOX, vs 89.3 ± 14.4%, scramble + MET + DOX) was abolished by presilencing FHC expression (22.5 ± 4.5%, siRNA FHC + MET + DOX) or NF-κB expression (24.4 ± 9.7%, siRNA NF-κB + MET + DOX). Consequently, ATP generation as a result of oxidative phosphorylation was also evaluated (Fig. 3). Treatment with DOX resulted in a significant decrease in ATP levels compared with the control (0.52 ± 0.05-fold of control, scramble + DOX). Pretreatment with MET prevented the DOX-mediated inhibition of ATP generation (1.3 ± 0.06, scramble + MET + DOX). The preventive effect of MET on ATP attenuation induced by DOX was completely blocked by prior silencing of FHC expression (0.57 ± 0.06, siRNA FHC + MET + DOX) or NF-κB (0.62 ± 0.01, siRNA NF-κB + MET + DOX). Compared with the respective controls, the silencing of FHC or NF-κB in the absence of treatment had no effect on complex I activity (Fig. 2B) or ATP generation (Fig. 3).

Identical treatments were conducted to evaluate the $\Delta\Psi$m, an important parameter of the mitochondrial function. To analyze this parameter we used the membrane-permeative dye JC-1, which changes its fluorescence emission from red to green when a loss of $\Delta\Psi$m occurs. The results of $\Delta\Psi$m analyses are shown in Fig. 4. Untreated HL-1 cells mainly emitted red fluorescence because most of the cell population was located in the R1 region (92.3 ± 9.1%, scr, Fig. 4A). When HL-1 cells were exposed to DOX, red fluorescence decreased and green fluorescence increased (Fig. 4B), with a subsequent diminution in the percentage of cells in the R1 region, which means a loss of $\Delta\Psi$m (15.2 ± 3.5%, scr + DOX). Pretreatment with MET 24 h before the addition of DOX prevented the diminution in the percentage of cells in the R1 region induced by DOX (75.5 ± 4.8%, scr + MET + DOX, Fig. 4C). Fig. 4D shows the kinetic of this decrease in the percentage of cells in the R1 region induced by DOX, and hence the kinetic of loss of $\Delta\Psi$m, which reached its lowest level after 15 h of treatment with DOX. The pretreatment with MET prevented this DOX-induced loss of $\Delta\Psi$m, whereas MET alone had no effect. The roles of FHC and

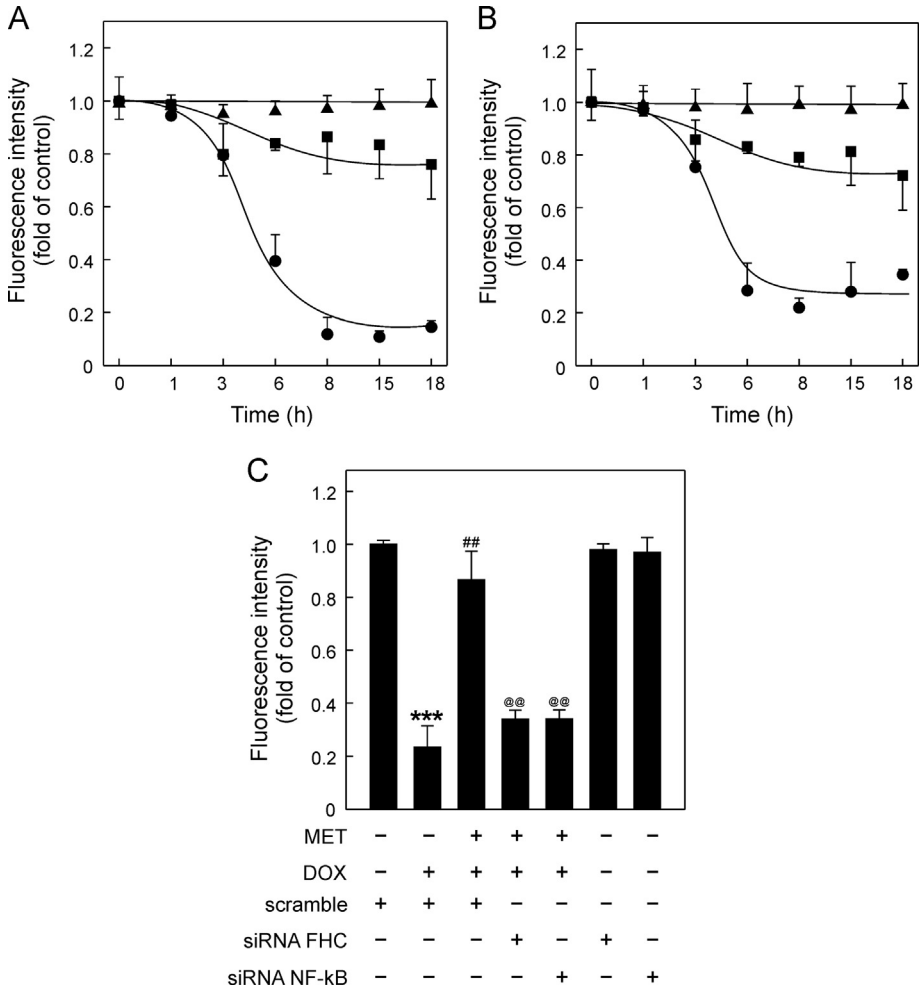

Fig. 1. MET, through NF-κB and FHC, prevents loss of DOX-induced iron homeostasis. (A and B) The cytosolic and mitochondrial free iron pools were measured using the fluorescent probes calcein-AM and RPA, respectively, as described under Materials and methods. The decrease in fluorescence intensity was used to calculate the increase in free iron pools. The cytosolic and mitochondrial free iron pools were determined in HL-1 cells treated with DOX alone (●) for the indicated treatment times or incubated with MET for 24 h before the addition of DOX (■). The effect of MET alone was also evaluated (▲). (C) HL-1 cardiomyocytes were preincubated with siRNA to scramble, FHC, or NF-κB before addition of DOX for 6 h alone or combined with a pretreatment with MET for 24 h. The effects of silencing FHC or NF-κB in the absence of treatment were also evaluated. Data are shown as the percentage of fluorescence with respect to the control (HL-1 cells with scramble alone). $^{***}p < 0.001$ vs scramble, $^{\#\#}p < 0.01$ vs scramble + DOX, $^{@@}p < 0.01$ vs scramble + MET + DOX.

NF-κB in the prevention of DOX-induced decrease in $\Delta\Psi$m by MET are shown in Fig. 4E. When the FHC or NF-κB expression was previously silenced using specific siRNAs, the preventive effect of MET was blocked (20.5 ± 4.8%, siRNA FHC + MET + DOX, or 21.6 ± 2.9%, siRNA NF-κB + MET + DOX). Compared with the respective controls, the presilencing of FHC or NF-κB in the absence of treatment had no significant effect. Finally, preincubation for 10 min with 5 μM cyclosporin A (CsA), a selective inhibitor of the MPTP, blocked the $\Delta\Psi$m changes induced by DOX (80.9 ± 2.6%, scr + CsA + DOX), whereas CsA had no effect on its own (95.6 ± 4.5%, scr + CsA). This indicates that the MPTP opening induced by DOX is responsible for $\Delta\Psi$m changes and that MET, via FHC and NF-κB, is able to prevent this opening.

MET prevents cytochrome c release and apoptosis induced by DOX

The $\Delta\Psi$m loss is seen in many forms of apoptosis and serves to link cytochrome *c* release and the activation of early initiator caspases with the activation of downstream effectors such as proteases and nucleases. Therefore, we next examined whether FHC and NF-κB are involved in the preventive effect of MET on the apoptosis induced by DOX in HL-1 cardiomyocytes. As shown in Fig. 5A, DOX induced cytochrome *c* release from mitochondria to the cytosol (6.54 ± 1.1-fold of control, scr + DOX), MET prevented this effect mediated by DOX (1.39 ± 0.2, scr + MET + DOX), and the presilencing of FHC or NF-κB blocked the preventive effect of MET (3.79 ± 0.4, siRNA FHC + MET + DOX, or 3.36 ± 0.3, siRNA NF-κB + MET + DOX). The activation of caspase 3 was also analyzed by Western blotting (Fig. 5B). Treatment of cardiomyocytes with DOX resulted in a significant activation of caspase 3 (5.9 ± 1.1-fold of control, scr + DOX). Pretreatment of cells with MET significantly inhibited DOX-induced caspase 3 activation (2.22 ± 0.6, scramble + MET + DOX), and the prior silencing of FHC or NF-κB also blocked the preventive effect of MET (6.51 ± 1.2, siRNA FHC + MET + DOX, or 6.65 ± 0.5, siRNA NF-κB + MET + DOX). The silencing of FHC or NF-κB in the absence of treatment had no effect on cytochrome *c* release or the activation of caspase 3. Analysis of DNA fragmentation by TUNEL assay (Fig. 6) showed an increase in the number of apoptotic cells induced by DOX compared with the control (71.3 ± 5.3%, scr + DOX, vs 6.5 ± 6.1%, scr), an increase that was suppressed by pretreatment with MET (15.5 ± 4.6%, scr + MET + DOX). Again, this preventive effect of MET was mediated by FHC and NF-κB because the effect was blocked by the presilencing of FHC (69.9 ± 9.3%, siRNA FHC + MET + DOX) or NF-κB (67.5 ± 6.6%, siRNA NF-κB + MET + DOX). The silencing of FHC or NF-κB in the absence of treatment had no effect on DNA fragmentation. Representative confocal microscopy images are shown in Supplementary Fig. 5.

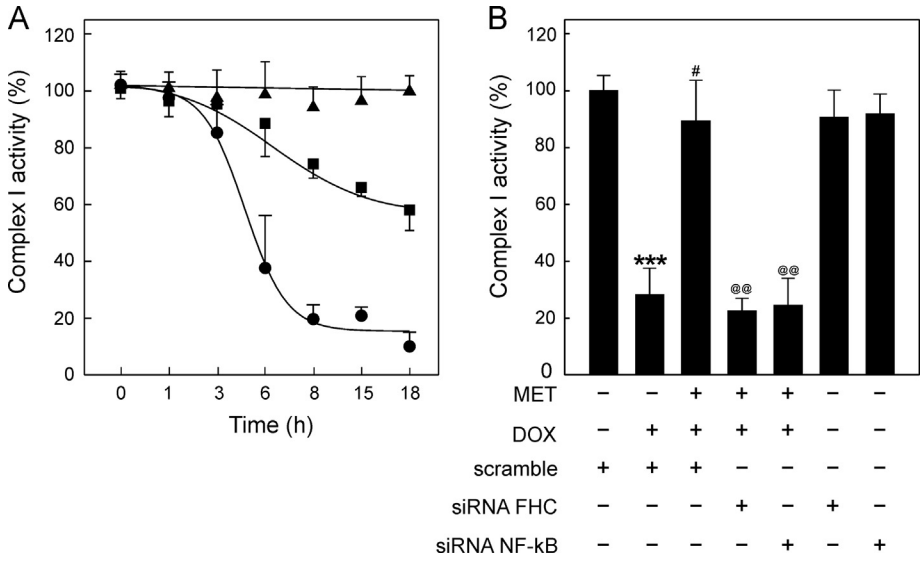

Fig. 2. MET, through NF-κB and FHC, prevents the inhibition of complex I induced by DOX. (A) The complex I activity was determined in HL-1 cells treated with DOX alone (•) for the indicated treatment times or with an incubation with MET for 24 h before addition of DOX (■). The effect of MET alone was also evaluated (▲). (B) HL-1 cardiomyocytes were preincubated with siRNA to scramble, FHC, or NF-κB before addition of DOX for 15 h alone or combined with a pretreatment with MET for 24 h. The effects of silencing FHC or NF-κB in the absence of treatments were also evaluated. Data are shown as the percentage of complex I activity with respect to the control (HL-1 cells with scramble alone). $^{***}p < 0.001$ vs scramble, $^{\#}p < 0.05$ vs scramble + DOX, $^{@@}p < 0.01$ vs scramble + MET + DOX.

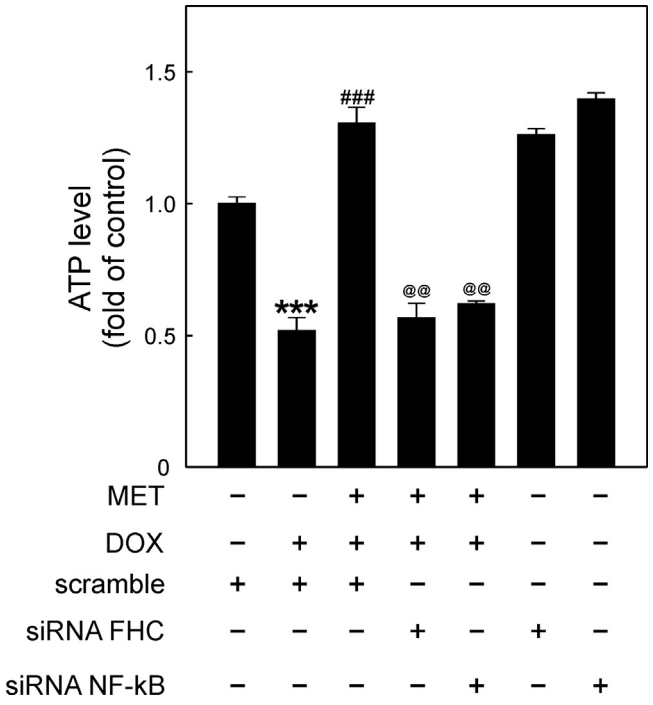

Fig. 3. MET, through NF-κB and FHC, prevents the inhibition of ATP synthesis mediated by DOX. HL-1 cells were preincubated with siRNA to scramble, FHC, or NF-κB before addition of DOX for 15 h alone or combined with a pretreatment with MET for 24 h. The effects of silencing FHC or NF-κB in the absence of treatments were also evaluated. The ATP generation was measured as described under Materials and methods and data are shown as fold of control (HL-1 cells with scramble alone). $^{***}p < 0.001$ vs scramble, $^{\#\#\#}p < 0.001$ vs scramble + DOX, $^{@@}p < 0.01$ vs scramble + MET + DOX.

Preventive effect of MET against DOX-induced damage in neonatal cardiomyocytes

The preventive effect of MET and the involvement of FHC and NF-κB were confirmed in a physiologically relevant experimental system using isolated primary neonatal rat cardiomyocytes. The effects on mitochondrial function and apoptosis were evaluated by conducting treatments identical to those described above. Fig. 7A shows the effect of treatments on the activity of complex I. The pretreatment with MET prevented the inhibition of complex I mediated by DOX (30.1 ± 3.62%, scr + DOX, vs 87.4 ± 4.25%, scr + MET + DOX). The preventive effect of MET was blocked by presilencing FHC expression (30.2 ± 3.21%, siRNA FHC + MET + DOX) or NF-κB expression (21.2 ± 3.25%, siRNA NF-κB + MET + DOX). Fig. 7B shows the effect of treatments on the $\Delta\Psi$m. The pretreatment with MET prevented the diminution in the percentage of cells in the R1 region induced by DOX and so prevented the loss of $\Delta\Psi$m (16.2 ± 5.63%, scr + DOX, vs 81.2 ± 4.23%, scr + MET + DOX). When the FHC or NF-κB expression was previously silenced, the preventive effect of MET was also blocked (19.4 ± 1.25%, siRNA FHC + MET + DOX, or 20.3 ± 3.25, siRNA NF-κB + MET + DOX). Finally, Fig. 7C and D show the effect of treatments on caspase 3 activity. Pretreatment of cells with MET significantly inhibited DOX-induced caspase 3 activation (5.8 ± 0.2, scr + DOX, vs 2.54 ± 0.4, scr + MET + DOX) and the prior silencing of FHC or NF-κB also blocked the preventive effect of MET (3.98 ± 0.3, siRNA FHC + MET + DOX, and 3.72 ± 0.5, siRNA NF-κB + MET + DOX). Compared to the control, the silencing of FHC or NF-κB in the absence of treatment had no effect on mitochondrial function or apoptosis.

Discussion

The main findings of this study are that MET was able to prevent the loss of iron homeostasis, mitochondrial dysfunction, and apoptosis induced by DOX in cardiomyocytes and that FHC and NF-κB are key molecules involved in this preventive role of MET. These findings suggest that FHC upregulation and, consequently, iron chelation are the main mechanisms responsible for the protective role of MET against DOX cardiotoxicity.

DOX-induced cardiotoxicity seems to be a multifactorial process and many mechanisms have been proposed and studied to explain it [32]. The most common hypothesis for the mechanism involved in DOX-induced cardiac injury is an increase in oxidative stress in the heart, manifested by an increase in free radical generation and usually associated with a depression of cardiac

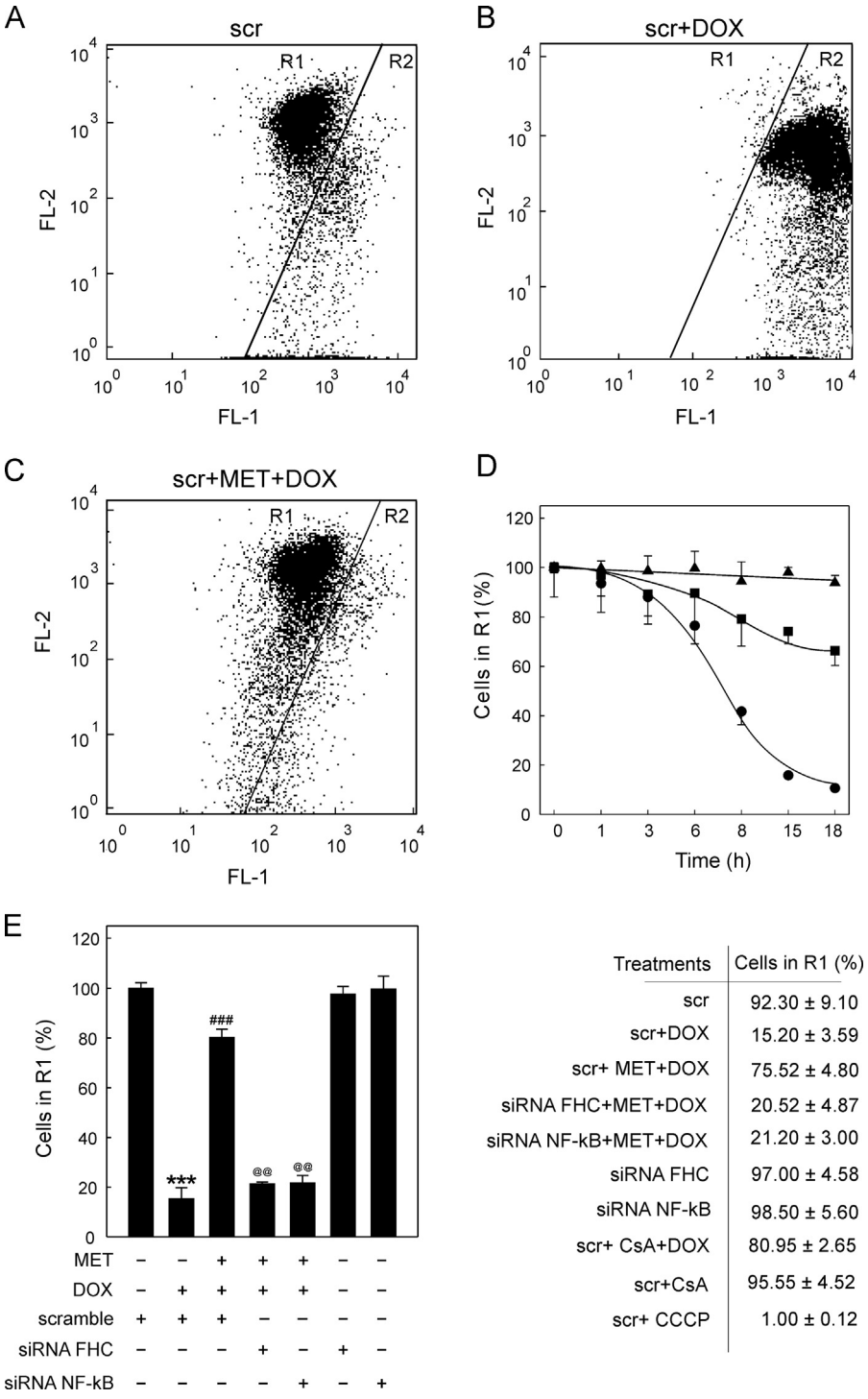

Treatments	Cells in R1 (%)
scr	92.30 ± 9.10
scr+DOX	15.20 ± 3.59
scr+ MET+DOX	75.52 ± 4.80
siRNA FHC+MET+DOX	20.52 ± 4.87
siRNA NF-kB+MET+DOX	21.20 ± 3.00
siRNA FHC	97.00 ± 4.58
siRNA NF-kB	98.50 ± 5.60
scr+ CsA+DOX	80.95 ± 2.65
scr+CsA	95.55 ± 4.52
scr+ CCCP	1.00 ± 0.12

Fig. 4. MET, through NF-κB and FHC, prevents loss of ΔΨm induced by DOX. To analyze ΔΨm we used the JC-1 dye, which changes its fluorescence emission from red to green when a loss of ΔΨm occurs. The green and red fluorescence of JC-1 was detected through the FL-1 and FL-2 channels, respectively. Cells with high and low ΔΨm are in region R1 and R2, respectively. Dot plots are representative of HL-1 after appropriate electronic gating: (A) untreated cells (scramble, scr), (B) treated with DOX alone for 15 h (scr + DOX), or (C) pretreated with MET 24 h before addition of DOX (scr + MET + DOX). (D) Time-dependent effects when cells were treated with DOX alone (●) or with an incubation with MET for 24 h before addition of DOX (■). The effect of MET alone was also evaluated (▲). (E) HL-1 cardiomyocytes were preincubated with siRNA to scramble, FHC, or NF-κB before addition of DOX for 15 h alone or combined with a pretreatment with MET for 24 h. Table shows means ± SD. Other controls were included: cyclosporin A (CsA; 5 μM, 10 min) is a selective inhibitor of the MPTP, and CCCP (5 μM, 30 min) is a proton ionophore that causes rapid mitochondrial membrane depolarization and therefore loss of ΔΨm. $^{***}p < 0.001$ vs scr, $^{\#\#\#}p < 0.001$ vs scr + DOX, $^{@@}p < 0.01$ vs scr + MET + DOX.

antioxidant systems [5,24]. This altered redox status causes damage in membranes, macromolecules, and mitochondria and may directly cause myocardial injury [24]. This hypothesis is supported by several reports that have shown that antioxidants, including vitamins E and A, resveratrol, or selenium, protect cardiomyocytes against the toxicity of DOX [17]. Iron homeostasis plays an important role in the DOX-induced oxidative stress in the heart. DOX itself has been shown to form a complex with iron, which catalyzes the conversion of hydrogen peroxide to the highly reactive hydroxyl radical [6,42]. In addition, DOX appears to perturb the iron homeostatic processes, which enhances ROS generation [33]. Dexrazoxane, an iron chelator, demonstrated clear

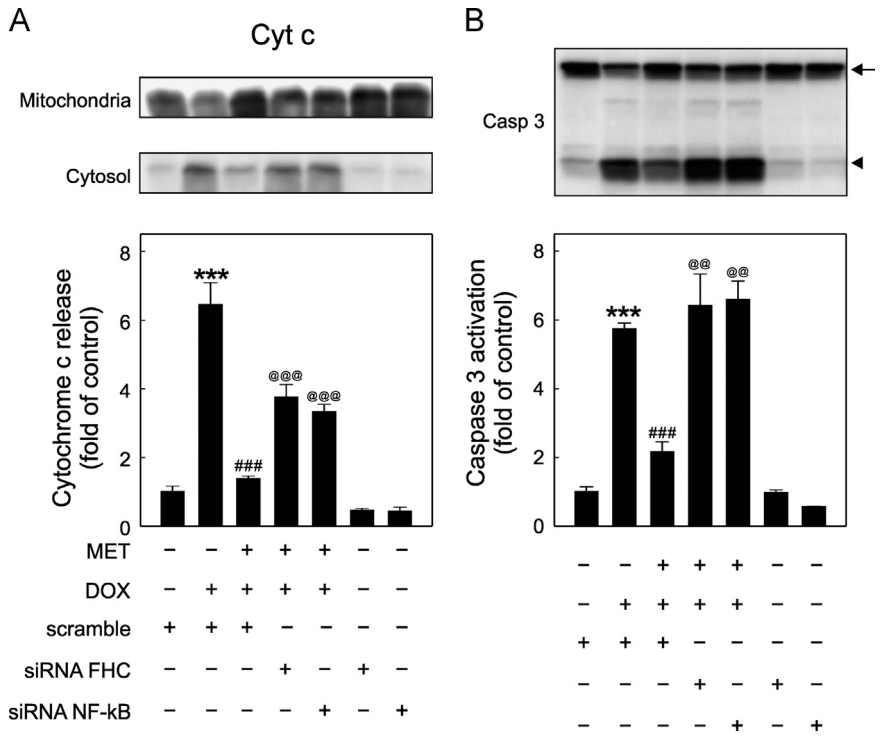

Fig. 5. MET, through NF-κB and FHC, prevents cytochrome *c* release and caspase 3 activation induced by DOX. (A) Representative Western blot of mitochondrial and cytosolic protein levels of cytochrome *c* in HL-1 cells preincubated with siRNA to scramble, FHC, or NF-κB before addition of the usual treatments with MET and/or DOX. The graph shows the densitometric data analysis of cytochrome *c* release calculated as the cytochrome *c* cytosol/mitochondria ratio and shown as fold of control (HL-1 cells with scramble alone). (B) Representative Western blot of caspase 3 (Casp 3) activation in HL-1 cells subjected to treatments identical to those described for (A). The densitometric data analysis was calculated as active caspase 3/procaspase. The uncleaved proform of caspase 3 is marked with an arrow and the active with an arrowhead. $^{***}p < 0.001$ vs scramble, $^{###}p < 0.001$ vs scramble + DOX, $^{@@}p < 0.01$, $^{@@@}p < 0.001$ vs scramble + MET + DOX.

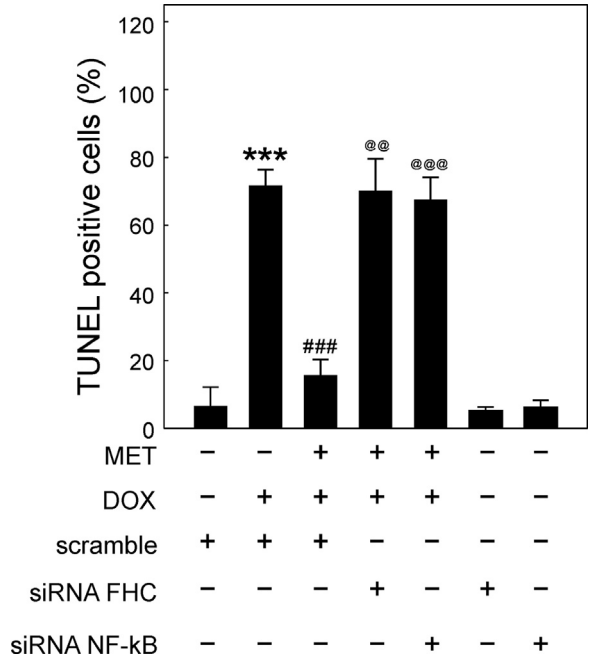

Fig. 6. MET, through NF-κB and FHC, prevents DNA fragmentation induced by DOX. HL-1 cells were preincubated with siRNA to scramble, FHC, or NF-κB before addition of the usual treatments with MET and/or DOX. The bar graph shows the percentage of TUNEL-positive HL-1 cells. $^{***}p < 0.001$ vs scramble, $^{###}p < 0.001$ vs scramble + DOX, $^{@@}p < 0.01$, $^{@@@}p < 0.001$ vs scramble + MET + DOX.

cardioprotective properties in clinical studies when administered before or with DOX [19,22,45]. However, the association of DOX, iron, and ROS is unclear, because other iron chelators, such as deferasirox, fail to exert the protective effects of dexrazoxane [21]. Our results showed simultaneous increases in cytosolic and mitochondrial free iron pools induced by DOX in cardiomyocytes, both of which were significant after 6 h of treatment with the anthracycline. These results are in good agreement with previous reports [12,28]. This increase in free iron pools induced by DOX was prevented by MET-mediated FHC upregulation, because the knockdown of FHC blocked the preventive effect of MET against the loss of iron homeostasis mediated by DOX. Previous results reported by our group showed that MET, via FHC upregulation, also prevents the oxidative stress induced by DOX in cardiomyocytes, which was demonstrated by the suppression of DOX-induced ROS generation and the restoration of cardiac antioxidant activities [5]. All these findings support the contribution and relationship of iron and ROS as mechanisms involved in DOX cardiotoxicity and suggest MET as a potential therapeutic agent against DOX-mediated cardiac injury. However, before we can translate the beneficial properties of MET to a clinical context, further in vivo studies are necessary to throw light on the role of MET in anthracycline cardiotoxicity and the importance of iron in this cardioprotective effect of MET.

The impairment of cardiac high-energy phosphate metabolism associated with a compromised mitochondrial function has been recognized as an important feature of both acute and chronic DOX cardiotoxic action [49]. The oxidative damage to cardiac mitochondria and to cardiomyocytes has been widely implicated as a primary cause of DOX-induced cardiac toxicity [31,54]. The enhanced generation of ROS by DOX may directly damage mitochondria or alter the synthesis of proteins associated with the mitochondrial electron transport chain, which inhibits oxidative phosphorylation and decreases cardiac high-energy phosphate homeostasis [7,55]. Our experimental model reproduced the mitochondrial dysfunction induced by DOX in cardiomyocytes,

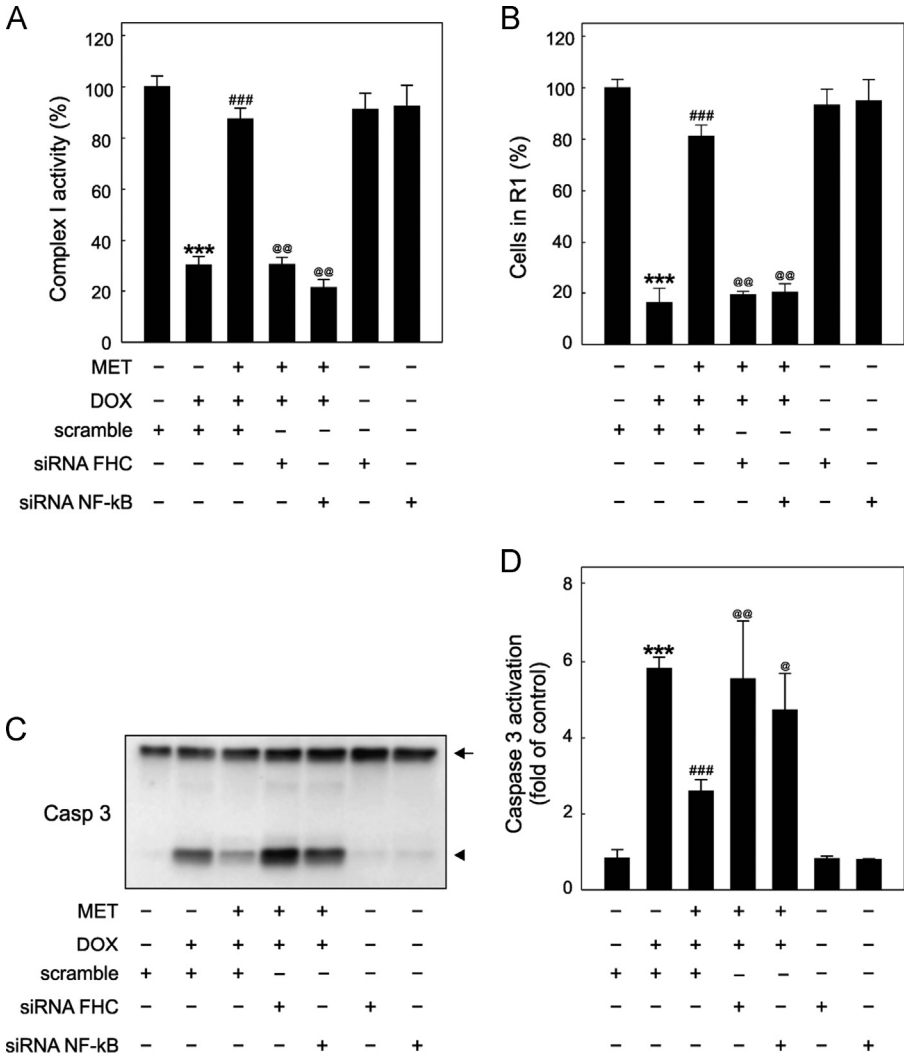

Fig. 7. The preventive effect of metformin against DOX-induced cardiotoxicity and the involvement of FHC and NF-κB were evaluated in isolated neonatal rat cardiomyocytes. The primary cells were subjected to treatments identical to those described earlier. The effects of treatments on (A) complex I activity, (B) ΔΨm, and (C and D) caspase 3 activation were evaluated as previously described for HL-1 cells. Casp 3, caspase 3. $^{***}p < 0.001$ vs scramble, $^{\#\#\#}p < 0.001$ vs scramble + DOX, $^{@}p < 0.05$, $^{@@}p < 0.01$ vs scramble + MET + DOX.

because DOX inhibited the activity of complex I of the mitochondrial electron transport chain and subsequently decreased ATP generation. In addition, our results show that MET prevents the mitochondrial dysfunction induced by DOX in cardiomyocytes, because MET blocked the inhibition of complex I mediated by DOX and restored ATP levels. Our results are in a good agreement with previous studies that showed the protective effect of MET against mitochondrial dysfunction in other experimental systems of cardiac injury such as ischemia–reperfusion, heart failure, or diabetes [8,18,52]. Recently, Ashour et al. [6] reported that MET may prevent DOX-induced cardiotoxicity in vivo by restoring ATP generation and intramitochondrial levels of CoA-SH, although the mechanism involved remains unclear. Our results show how MET, through the NF-κB-mediated upregulation of FHC, is able to prevent the increase in cytosolic and mitochondrial free iron pools induced by DOX in cardiomyocytes. Moreover, the knockdown of NF-κB or FHC also blocked the protective effect of MET against the inhibition of complex I and energy starvation induced by DOX in cardiomyocytes. These results reveal that the restoration of iron homeostasis is a key mechanism involved in the cardioprotective role of MET against mitochondrial dysfunction induced by DOX and therefore against its cardiotoxicity.

Mitochondrial dysfunction has been shown to participate in DOX-mediated cardiomyocyte death by inducing the apoptotic pathway [42]. Indeed, MPTP opening has been demonstrated to induce the depolarization of ΔΨm, the release of apoptogenic factors, the activation of caspases, and DNA damage [29,42]. The results obtained in this study confirm all these cardiotoxic effects of DOX in HL-1 cells and demonstrate that MET prevents the loss of ΔΨm, the release of cytochrome *c*, caspase activation, and DNA damage induced by DOX. It is frequently suggested that iron is involved in DOX-induced cardiac apoptosis, and some iron chelators, such as dexrazoxane or desferrioxamine, have shown a preventive effect against DOX-induced apoptosis in experimental models [3,22,45]; however, others, such as Dp44mT, failed to offer such protection [20]. In this study, the silencing of FHC blocked the preventive effect of MET on the loss of ΔΨm and apoptosis induced by DOX, which confirms the involvement of iron in the DOX-induced apoptosis in cardiomyocyte and its key role in the antiapoptotic effect of MET against DOX cardiotoxicity.

Because of the undisputed key role that DOX plays in the treatment of many neoplastic diseases, one of the aims being pursued most intensively is the possibility of eliminating its cardiotoxicity or reducing the same to an acceptable level. If the

cardiac complications resulting from DOX could be prevented, or at least reduced, higher doses could potentially be used, thereby increasing cancer cure rates. In this regard, various drugs, including L-carnitine [11] or dexrazoxane [19], have been shown to protect against DOX-induced cardiotoxicity. The results of this study suggest MET could be used as a potential therapeutic drug against the cardiotoxic effects of DOX. In addition to its low toxicity and low cost, MET therapy could have an advantage over iron-chelator therapies, because MET-induced FHC upregulation mimics the physiological response of cardiomyocytes to the increase in ROS levels induced by DOX [9]. In addition, MET does not reduce the antitumor activity of DOX and could work synergistically with it to reduce tumor growth and prevent relapse in a broad variety of cancer types [14,23,25]. The cardioprotective action of MET has been demonstrated in preclinical and clinical studies [1,2,13,41]. However, to date, no studies or clinical trials have tried to assess the cardioprotective role of MET in cardiac damage patients receiving DOX. The findings presented here support this hypothesis. These results were obtained in the HL-1 cell line and in cardiomyocyte primary culture, which have allowed us to characterize the cardioprotective effect of MET against DOX-induced cardiotoxicity in the absence of confounding factors, such as hormonal and inflammatory response. However, further experiments using an in vivo model are mandatory to confirm MET protection in a physiologic context.

Acknowledgments

This study was supported in part by Grant 11857/PI/09 (to D.A. P.-F.) from the Fundación Séneca, Murcia, Spain; by Grant PS09/02106 (to M.V.) from the Ministerio de Sanidad, Madrid, Spain; and by the National Network of Investigation in Cardiovascular Diseases (RD12/0042/0049).

Appendix A. Supporting information

Supplementary data associated with this article can be found in the online version at XX

References

[1] U.K. Prospective Diabetes Study Group. Effect of intensive blood-glucose control with metformin on complications in overweight patients with type 2 diabetes (UKPDS 34). *Lancet* **352:**854–865; 1998.
[2] U.K. Prospective Diabetes Study Group. UKPDS 28: a randomized trial of efficacy of early addition of metformin in sulfonylurea-treated type 2 diabetes. *Diabetes Care* **21:**87–92; 1998.
[3] Al-Shabanah, O. A.; Aleisa, A. M.; Hafez, M. M.; Al-Rejaie, S. S.; Al-Yahya, A. A.; Bakheet, S. A., et al. Desferrioxamine attenuates doxorubicin-induced acute cardiotoxicity through TFG-beta/Smad p53 pathway in rat model. *Oxid. Med. Cell. Longevity* **2012:**619185; 2012.
[4] Asensio-Lopez, M. C.; Lax, A.; Pascual-Figal, D. A.; Valdes, M.; Sanchez-Mas, J. Metformin protects against doxorubicin-induced cardiotoxicity: involvement of the adiponectin cardiac system. *Free Radic. Biol. Med.* **51:**1861–1871; 2011.
[5] Asensio-Lopez, M. C.; Sanchez-Mas, J.; Pascual-Figal, D. A.; Abenza, S.; Perez-Martinez, M. T.; Valdes, M., et al. Involvement of ferritin heavy chain in the preventive effect of metformin against doxorubicin-induced cardiotoxicity. *Free Radic. Biol. Med.* **57:**188–200; 2013.
[6] Ashour, A. E.; Sayed-Ahmed, M. M.; Abd-Allah, A. R.; Korashy, H. M.; Maayah, Z. H.; Alkhalidi, H., et al. Metformin rescues the myocardium from doxorubicin-induced energy starvation and mitochondrial damage in rats. *Oxid. Med. Cell. Longevity* **2012:**434195; 2012.
[7] Berthiaume, J. M.; Wallace, K. B. Adriamycin-induced oxidative mitochondrial cardiotoxicity. *Cell. Biol. Toxicol.* **23:**15–25; 2007.
[8] Bhamra, G. S.; Hausenloy, D. J.; Davidson, S. M.; Carr, R. D.; Paiva, M.; Wynne, A. M., et al. Metformin protects the ischemic heart by the Akt-mediated inhibition of mitochondrial permeability transition pore opening. *Basic Res. Cardiol.* **103:**274–284; 2008.
[9] Corna, G.; Santambrogio, P.; Minotti, G.; Cairo, G. Doxorubicin paradoxically protects cardiomyocytes against iron-mediated toxicity: role of reactive oxygen species and ferritin. *J. Biol. Chem.* **279:**13738–13745; 2004.
[10] Cossarizza, A.; Baccarani-Contri, M.; Kalashnikova, G.; Franceschi, C. A new method for the cytofluorimetric analysis of mitochondrial membrane potential using the J-aggregate forming lipophilic cation 5,5′,6,6′-tetrachloro-1,1′,3,3′-tetraethylbenzimidazolcarbocyanine iodide (JC-1). *Biochem. Biophys. Res. Commun.* **197:**40–45; 1993.
[11] De, L. V.; Neri, B.; Bacalli, S.; Cinelli, P. Reduction of cardiac toxicity of anthracyclines by L-carnitine: preliminary overview of clinical data. *Int. J. Clin. Pharmacol. Res.* **5:**137–142; 1985.
[12] Elliott, A. M.; Al-Hajj, M. A. ABCB8 mediates doxorubicin resistance in melanoma cells by protecting the mitochondrial genome. *Mol. Cancer Res.* **7:**79–87; 2009.
[13] Eurich, D. T.; Majumdar, S. R.; McAlister, F. A.; Tsuyuki, R. T.; Johnson, J. A. Improved clinical outcomes associated with metformin in patients with diabetes and heart failure. *Diabetes Care* **28:**2345–2351; 2005.
[14] Feng, Y. H.; Velazquez-Torres, G.; Gully, C.; Chen, J.; Lee, M. H.; Yeung, S. C. The impact of type 2 diabetes and antidiabetic drugs on cancer cell growth. *J. Cell. Mol. Med.* **15:**825–836; 2011.
[15] Gianni, L.; Vigano, L.; Locatelli, A.; Capri, G.; Giani, A.; Tarenzi, E., et al. Human pharmacokinetic characterization and in vitro study of the interaction between doxorubicin and paclitaxel in patients with breast cancer. *J. Clin. Oncol.* **15:**1906–1915; 1997.
[16] Gianni, L.; Zweier, J. L.; Levy, A.; Myers, C. E. Characterization of the cycle of iron-mediated electron transfer from Adriamycin to molecular oxygen. *J. Biol. Chem.* **260:**6820–6826; 1985.
[17] Granados-Principal, S.; Quiles, J. L.; Ramirez-Tortosa, C. L.; Sanchez-Rovira, P.; Ramirez-Tortosa, M. C. New advances in molecular mechanisms and the prevention of Adriamycin toxicity by antioxidant nutrients. *Food Chem. Toxicol.* **48:**1425–1438; 2010.
[18] Gundewar, S.; Calvert, J. W.; Jha, S.; Toedt-Pingel, I.; Ji, S. Y.; Nunez, D., et al. Activation of AMP-activated protein kinase by metformin improves left ventricular function and survival in heart failure. *Circ. Res.* **104:**403–411; 2009.
[19] Hasinoff, B. B.; Herman, E. H. Dexrazoxane: how it works in cardiac and tumor cells. Is it a prodrug or is it a drug? *Cardiovasc. Toxicol.* **7:**140–144; 2007.
[20] Hasinoff, B. B.; Patel, D. The iron chelator Dp44mT does not protect myocytes against doxorubicin. *J. Inorg. Biochem.* **103:**1093–1101; 2009.
[21] Hasinoff, B. B.; Patel, D.; Wu, X. The oral iron chelator ICL670A (deferasirox) does not protect myocytes against doxorubicin. *Free Radic. Biol. Med.* **35:**1469–1479; 2003.
[22] Hasinoff, B. B.; Schnabl, K. L.; Marusak, R. A.; Patel, D.; Huebner, E. Dexrazoxane (ICRF-187) protects cardiac myocytes against doxorubicin by preventing damage to mitochondria. *Cardiovasc. Toxicol.* **3:**89–99; 2003.
[23] Hirsch, H. A.; Iliopoulos, D.; Tsichlis, P. N.; Struhl, K. Metformin selectively targets cancer stem cells, and acts together with chemotherapy to block tumor growth and prolong remission. *Cancer Res.* **69:**7507–7511; 2009.
[24] Horenstein, M. S.; Vander Heide, R. S.; L'Ecuyer, T. J. Molecular basis of anthracycline-induced cardiotoxicity and its prevention. *Mol. Genet. Metab.* **71:**436–444; 2000.
[25] Iliopoulos, D.; Hirsch, H. A.; Struhl, K. Metformin decreases the dose of chemotherapy for prolonging tumor remission in mouse xenografts involving multiple cancer cell types. *Cancer Res.* **71:**3196–3201; 2011.
[26] Kaiserova, H.; Simunek, T.; Sterba, M.; den Hartog, G. J.; Schroterova, L.; Popelova, O., et al. New iron chelators in anthracycline-induced cardiotoxicity. *Cardiovasc. Toxicol.* **7:**145–150; 2007.
[27] Kewalramani, G.; Puthanveetil, P.; Wang, F.; Kim, M. S.; Deppe, S.; Abrahani, A., et al. AMP-activated protein kinase confers protection against TNF-{alpha}-induced cardiac cell death. *Cardiovasc. Res.* **84:**42–53; 2009.
[28] Kwok, J. C.; Richardson, D. R. Examination of the mechanism(s) involved in doxorubicin-mediated iron accumulation in ferritin: studies using metabolic inhibitors, protein synthesis inhibitors, and lysosomotropic agents. *Mol. Pharmacol.* **65:**181–195; 2004.
[29] L'Ecuyer, T.; Sanjeev, S.; Thomas, R.; Novak, R.; Das, L.; Campbell, W., et al. DNA damage is an early event in doxorubicin-induced cardiac myocyte death. *Am. J. Physiol. Heart Circ. Physiol.* **291:**H1273–H1280; 2006.
[30] Lax, A.; Soler, F.; Fernandez-Belda, F. Mitochondrial damage as death inducer in heart-derived H9c2 cells: more than one way for an early demise. *J. Bioenerg. Biomembr.* **41:**369–377; 2009.
[31] Lee, V.; Randhawa, A. K.; Singal, P. K. Adriamycin-induced myocardial dysfunction in vitro is mediated by free radicals. *Am. J. Physiol.* **261:** H989–H995; 1991.
[32] Minotti, G.; Menna, P.; Salvatorelli, E.; Cairo, G.; Gianni, L. Anthracyclines: molecular advances and pharmacologic developments in antitumor activity and cardiotoxicity. *Pharmacol. Rev.* **56:**185–229; 2004.
[33] Minotti, G.; Recalcati, S.; Mordente, A.; Liberi, G.; Calafiore, A. M.; Mancuso, C., et al. The secondary alcohol metabolite of doxorubicin irreversibly inactivates aconitase/iron regulatory protein-1 in cytosolic fractions from human myocardium. *FASEB J.* **12:**541–552; 1998.
[34] Miranda, C. J.; Makui, H.; Soares, R. J.; Bilodeau, M.; Mui, J.; Vali, H., et al. Hfe deficiency increases susceptibility to cardiotoxicity and exacerbates changes in iron metabolism induced by doxorubicin. *Blood* **102:**2574–2580; 2003.
[35] Mott, M. G. Anthracycline cardiotoxicity and its prevention. *Ann. N. Y. Acad. Sci.* **824:**221–228; 1997.

[36] Owen, M. R.; Doran, E.; Halestrap, A. P. Evidence that metformin exerts its anti-diabetic effects through inhibition of complex 1 of the mitochondrial respiratory chain. *Biochem. J.* **348(Pt 3):**607–614; 2000.
[37] Rauen, U.; Springer, A.; Weisheit, D.; Petrat, F.; Korth, H. G.; de, G. H., et al. Assessment of chelatable mitochondrial iron by using mitochondrion-selective fluorescent iron indicators with different iron-binding affinities. *Chembiochem* **8:**341–352; 2007.
[38] Sardao, V. A.; Pereira, S. L.; Oliveira, P. J. Drug-induced mitochondrial dysfunction in cardiac and skeletal muscle injury. *Expert Opin. Drug Saf.* **7:**129–146; 2008.
[39] Sasaki, H.; Asanuma, H.; Fujita, M.; Takahama, H.; Wakeno, M.; Ito, S., et al. Metformin prevents progression of heart failure in dogs: role of AMP-activated protein kinase. *Circulation* **119:**2568–2577; 2009.
[40] Sawaya, H.; Sebag, I. A.; Plana, J. C.; Januzzi, J. L.; Ky, B.; Cohen, V., et al. Early detection and prediction of cardiotoxicity in chemotherapy-treated patients. *Am. J. Cardiol.* **107:**1375–1380; 2011.
[41] Shah, D. D.; Fonarow, G. C.; Horwich, T. B. Metformin therapy and outcomes in patients with advanced systolic heart failure and diabetes. *J. Card. Fail.* **16:**200–206; 2010.
[42] Simunek, T.; Sterba, M.; Popelova, O.; Adamcova, M.; Hrdina, R.; Gersl, V. Anthracycline-induced cardiotoxicity: overview of studies examining the roles of oxidative stress and free cellular iron. *Pharmacol. Rep.* **61:**154–171; 2009.
[43] Singal, P. K.; Iliskovic, N. Doxorubicin-induced cardiomyopathy. *N. Engl. J. Med.* **339:**900–905; 1998.
[44] Soler, F.; Lax, A.; Fernandez-Belda, F. Cellular death linked to irreversible stress in the sarcoplasmic reticulum: the effect of inhibiting Ca^{2+}-ATPase or protein glycosylation in the myocardiac cell model H9c2. *Arch. Biochem. Biophys.* **466:**194–202; 2007.
[45] Spagnuolo, R. D.; Recalcati, S.; Tacchini, L.; Cairo, G. Role of hypoxia-inducible factors in the dexrazoxane-mediated protection of cardiomyocytes from doxorubicin-induced toxicity. *Br. J. Pharmacol.* **163:**299–312; 2011.
[46] Swain, S. M.; Whaley, F. S.; Ewer, M. S. Congestive heart failure in patients treated with doxorubicin: a retrospective analysis of three trials. *Cancer* **97:**2869–2879; 2003.
[47] Thomas, C. E.; Aust, S. D. Release of iron from ferritin by cardiotoxic anthracycline antibiotics. *Arch. Biochem. Biophys.* **248:**684–689; 1986.
[48] Torti, F. M.; Torti, S. V. Regulation of ferritin genes and protein. *Blood* **99:**3505–3516; 2002.
[49] Wallace, K. B. Doxorubicin-induced cardiac mitochondrionopathy. *Pharmacol. Toxicol.* **93:**105–115; 2003.
[50] Wallace, K. B. Adriamycin-induced interference with cardiac mitochondrial calcium homeostasis. *Cardiovasc. Toxicol.* **7:**101–107; 2007.
[51] Walter, P. B.; Knutson, M. D.; Paler-Martinez, A.; Lee, S.; Xu, Y.; Viteri, F. E., et al. Iron deficiency and iron excess damage mitochondria and mitochondrial DNA in rats. *Proc. Natl. Acad. Sci. USA* **99:**2264–2269; 2002.
[52] Whittington, H. J.; Hall, A. R.; McLaughlin, C. P.; Hausenloy, D. J.; Yellon, D. M.; Mocanu, M. M. Chronic metformin associated cardioprotection against infarction: not just a glucose lowering phenomenon. *Cardiovasc. Drugs Ther.* **27:**5–16; 2013.
[53] Wouters, K. A.; Kremer, L. C.; Miller, T. L.; Herman, E. H.; Lipshultz, S. E. Protecting against anthracycline-induced myocardial damage: a review of the most promising strategies. *Br. J. Haematol.* **131:**561–578; 2005.
[54] Xu, M. F.; Tang, P. L.; Qian, Z. M.; Ashraf, M. Effects by doxorubicin on the myocardium are mediated by oxygen free radicals. *Life Sci.* **68:**889–901; 2001.
[55] Zhou, S.; Palmeira, C. M.; Wallace, K. B. Doxorubicin-induced persistent oxidative stress to cardiac myocytes. *Toxicol. Lett.* **121:**151–157; 2001.